

14. Wilkinson D. Calculation of Blade-to-Blade Flow in a Turbomachine by Streamline Curvature // Reports and Memoranda No. 3704. 1970. URL: <http://naca.central.cranfield.ac.uk/reports/arc/rm/3704.pdf>
15. Flow characteristics on the blade channel vortex in the Francis turbine / Guo P. C., Wang Z. N., Luo X. Q., Wang Y. L., Zuo J. L. // IOP Conference Series: Materials Science and Engineering. 2016. Vol. 129. P. 012038. doi: <https://doi.org/10.1088/1757-899x/129/1/012038>

Запропоновано схему гібридної відновлюваної електричної станції з розширеним використанням встановленого обладнання гідроакумуляуючого блоку для перетворення постійного струму фотоелектричних та вітрових генераторів в змінний.

Схема базується на наявних компонентах з широко використовуваною відпрацьованою технологією. Для видачі потужності та перетворення постійного струму сонячних та вітрових генераторів в змінний окрім мережевих інверторів використовується синхронний генератор гідроакумуляуючого блоку. Для обертання генератора крім гідротурбіни також використовується асинхронний двигун, підключений через частотно-регульований привод до загальної шини постійного струму станції. Крім того, до шини постійного струму підключені електрохімічні акумулятори і батареї конденсаторів.

Проаналізовано можливість використання різних типів електричних машин для приводу синхронного генератора і показано перевагу асинхронного двигуна. Змодельовано реакцію асинхронного двигуна на коливання швидкості обертання і показано його здатність брати участь в регулюванні частоти мережі. На прикладі типового добового графіка навантаження і генерації показано, що запропоноване рішення по перетворенню постійного струму в змінний має ККД, близький до ККД мережевого інвертора.

Запропонована схема гібридної станції дозволяє підвищити надійність роботи відновлюваних джерел енергії і стабільність частоти мережі. Це досягається завдяки збільшенню інерції обертючих мас в енергосистемі, можливості управління коефіцієнтом потужності синхронного генератора і властивій асинхронному двигуну реакції на коливання швидкості обертання. Створення таких гібридних станцій відкриває шлях до подальшого збільшення частки відновлюваних джерел в енергосистемі

Ключові слова: відновлювана енергетика, гібридна електростанція, частотно-регульований привод, асинхронний двигун

UDC 620.91

DOI: 10.15587/1729-4061.2019.160531

DEVELOPMENT OF A RENEWABLE HYBRID POWER PLANT WITH EXTENDED UTILIZATION OF PUMPED STORAGE UNIT EQUIPMENT

K. Makhotilo

PhD, Professor, Senior Researcher*

E-mail: kvmahotilo@gmail.com**I. Chervonenko**

PhD, Associate Professor*

E-mail: iichervonenko@gmail.com**A. H. Saad El Masri**

Postgraduate Student*

E-mail: allensaad@gmail.com

*Department of Electric Power Stations

National Technical University

«Kharkiv Polytechnic Institute»

Kyrpychova str., 2, Kharkiv,

Ukraine, 61002

1. Introduction

Electrical power generation is changing dramatically around the world. The installed capacity of wind and solar power plants is already measured in hundreds of GW. Currently, mainly maneuverable gas turbine units and pumped-storage power plants (PSPP) are used to compensate the negative impact of renewable energy (RE) sources on the stability of the power system. In recent years, we can see accelerated growth of different kinds of renewable hybrid power plants (RHPP) which can incorporate photovoltaic systems, wind generators and powerful Li-Ion storage battery units.

This promising technology ensures stable generation of electricity and high maneuverability level of RHPP but it still

has a number of drawbacks. On the other hand, more traditional RHPP schemes including those that use small PSPP for energy accumulation are also explored in the world. The true potential of this type of plants has not yet been fully shown; and they can solve the problems that we will encounter as the use of Li-Ion storage batteries in power systems increases.

2. Literature review and problem statement

In power grids, electronically coupled sources have been growing rapidly over the past few years, where the reliability of stable power balance between generation and demand is achieved by the sole use of energy storage [1].

In hybrid Wind/Solar renewable power plants, energy storage is mainly available in the presence of Li-Ion batteries, which need to be optimized in ratings to deliver maximum operational and financial benefits [2].

The DC to AC conversion units play a very important role in RE generation. With the continuous technological improvement and the emergence of reliable high-efficiency DC/AC grid inverters (and now with the capability to incorporate the power factor control), grid inverters seemed to be the only appropriate solution for powering AC grids from RE sources. However, in most cases, grid inverters do not provide inertial response and, therefore, tend to alter the transient frequency response of power systems [3].

The rotation kinetic energy reserve remains the key for handling transient disturbances affecting power grid reliability. Actually, any transient disturbance in load balance between the generated and consumed power results in changes in AC grids frequency f above or below its rated value f_0 . The resulting frequency deviation Δf is mostly compensated for by fast changes in the kinetic energy of the rotating electric machines connected to the grid. The time derivative of the frequency deviation Δf can be estimated as follows [4]:

$$\frac{d(\Delta f(t))}{dt} = f_0 \frac{P_g(t) - P_l(t)}{2E_m}, \quad (1)$$

where $P_g(t)$ – the generated power and $P_l(t)$ – the load requirement, and E_m – the kinetic energy of the rotating electric machines.

Accordingly, it is well clear that the rate of change in grid frequency is inversely proportional to the magnitude of the kinetic energy of the rotating electric machines.

In limited/isolated power grids, rotating generators are few in quantity and form a significant percentage of the overall power generation capability. As the installed capacity of RE sources increases, synchronous units must be dispatched down and eventually shut down when their minimum power output is reached. This reduces the overall power system inertia [1], with less kinetic energy E_m proportional to the power of remaining rotating electric machines connected to the grid.

The result is leaving the grid more vulnerable to frequency disturbances in view of the negligible inertial response of RE sources. Noting that RE on-grid inverters protection circuitry is designed to isolate the inverters against low grid frequencies, this can worsen more the power system reliability when for some reasons frequency drops. This results in the relatively frequent use of automatic load-shedding (ALS) to restore the power equilibrium and prevent frequency collapse, with subsequent consequences on the economic activity, among others [1].

To prevent the development of such a negative scenario, a number of solutions are used.

The most common approach is to limit the maximum level of using RE sources in the power system or to introduce additional rotating masses, for example, by switching the generators to the synchronous compensator mode [5]. However, this approach worsens the power system economic performance due to additional costs or the partial loss of the available «free» energy.

Pumped storage units, when incorporated in hybrid «renewable energy generation plants, can enhance the inertial response of the power grid, provide an unlimited number of charge/discharge cycles and the high rate of installed capacity [6]. PSPPs support a deeper penetration of RE sources into

the power system, but today they cannot operate in the primary frequency control mode due to an insufficiently fast start [7].

Distributed energy storage systems based on Li-Ion batteries or supercapacitors have a higher reaction speed, are able to compensate fluctuations in the power of renewable energy sources, and provide dynamic frequency control [8]. However, the cost and immature technology of such devices, as well as limited service life, significantly restrict the possibility of wide application of such systems.

Another solution is the electronically coupled sources able to mimic the rotational inertia of conventional generators in power systems with a large share of inverters [9]. For example, variable speed wind turbines can supply synthetic inertia thanks to a supplementary loop in their control system [10]. However, ensuring the required quality of electric energy, in particular, compensation of higher harmonics, remains an unresolved problem when using this solution [11].

Thus, none of the presented solutions is ideal. All of them suffer from complex implementations, high costs, or immaturity of technology. This necessitates finding new ways to increase the use of RE in the power systems.

3. The aim and objectives of the study

The aim is to propose a RHPP scheme based on hydro pumped storage plant, which allows to partially or completely replace the grid inverters with electrical machines, thus extend the utilization of PSPP equipment and reduce the negative impact of renewable energy sources on the electric power grid.

To do this, it is necessary to accomplish the following objectives:

- to propose, as an alternative to the exclusive use of inverters for renewable energy sources, a solution for DC to AC conversions using the existing equipment of the pumped storage unit of RHPP;
- to simulate various operating modes of the RHPP equipment, to estimate the possibility of participating in frequency control and the efficiency of the proposed solution, and to show the possibility of increasing the share of renewable energy generation in the power system.

4. Improving of the renewable hybrid power plant scheme

4.1. Conventional renewable hybrid power plant scheme

Fig. 1 shows a common scheme of RHPP, with the photovoltaic system (PV) and wind generator (WG) connected to the electric power grid, along with an independently controlled pumped-storage hydropower plant acting as a power generating unit during hours of daily grid load peaks or continuous lowering of PV and WG power output. The PSPP pumps the water to the upper reservoir during off-peak hours or during times of excess solar/wind RE power generation, thus acting as load draining its power from the power grid. In Fig. 1, MPPT stands for PV system maximum power point tracker, INV for power inverter and SM for the synchronous machine.

This scheme achieves a controlled power output of RHPP in the simplest way. However, it has its limitations for maintaining a certain constant level of output power at times of availability of high power generated from solar and wind plants, especially when the PSPP is disconnected or used in the pumping mode. Furthermore, though the PSPP when

powered-on offers the possibility to regulate the output power, there are also limitations on the response speed involved in the power regulation process.

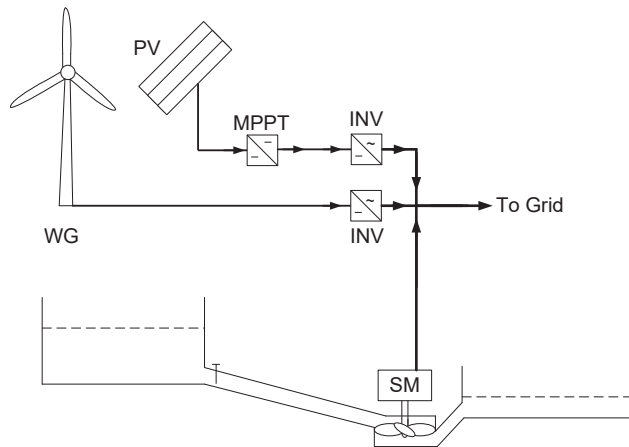


Fig. 1. Conventional RHPP configuration

4. 2. Renewable hybrid power plant scheme with a common DC bus

The RHPP scheme in Fig. 2 shows a possible improvement in the common RHPP scheme. It introduces an intermediate DC bus and limited storage battery (BAT) and capacitor banks (C) that can power the DC/AC inverters, thus serving as an intermediate energy pool. As compared to the initial conventional configuration in Fig. 1, the extended configuration allows using one common inverter. With the use of DC bus, this scheme can instantaneously compensate transient fluctuations in the solar and wind power outputs, and can allow absorbing peaks in RE sources. This makes it possible to increase the use of potentially available power from RE sources. In Fig. 2, REC stands for DC rectifier.

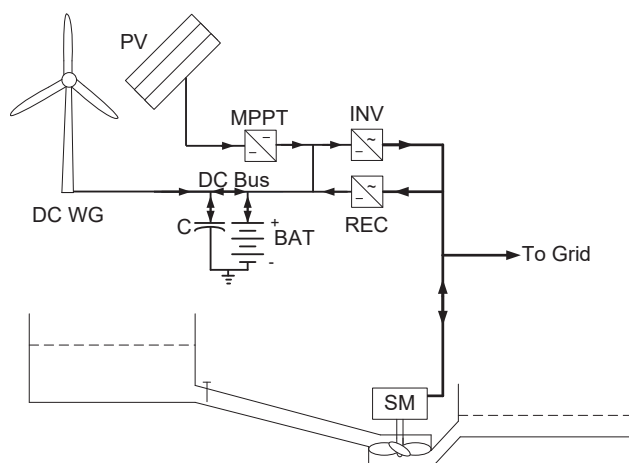


Fig. 2. RHPP configuration with common DC bus, batteries and ultracapacitors

Ultracapacitors [12, 13] are well suited to pulse power applications [1], with their low impedance can further improve the DC system efficiency, and can reduce momentary strain on batteries. For example, MW-scale ultra-capacitor based distributed storage system was built in Hawaii in 2006. It counteracted the power and voltage fluctuations of a wind farm and improved significantly the grid stability [14].

The RHPP configuration in Fig. 2 offers much more output AC power stability for RE power sources than the standard configuration. However, there are still certain problems that need to be addressed:

- the harmonics introduced to the power system by the grid inverter. Harmonics are well known to have undesirable effects on the performance of certain grid components such as power transformers windings. In addition, harmonics can result in premature failure of AC power factor correction capacitors if they are not suited for such application, i. e. not containing current limiting reactors or thyristor-controlled reactors;
- the RE on-grid inverters protection circuitry. Designed to isolate the inverters against low grid frequencies, it would pose a potential problem to grid reliability in isolating the inverters when their power is needed to support load balance;
- high transient currents consumed by the hydro storage synchronous machine when started from the grid power in the motor mode. The high currents of low power factor nature can cause undesirable grid lines voltage fluctuations (mainly voltage drops) for a significant amount of time until certain synchronous rotational speed is attained by the motor.

4. 3. Renewable hybrid power plant scheme with extended utilization of hydro generator

The RHPP configuration in Fig. 3 offers advantages over the previous ones, it also resolves the issues of concern above. Instead of using a grid DC/AC inverter as the only means to power the grid, it is proposed to extend the utilization of pumped storage unit equipment. The existing power synchronous generator/machine (SM) can be used for DC to AC conversion by coupling it to an electric motor powered from the common DC bus through the electric drive.

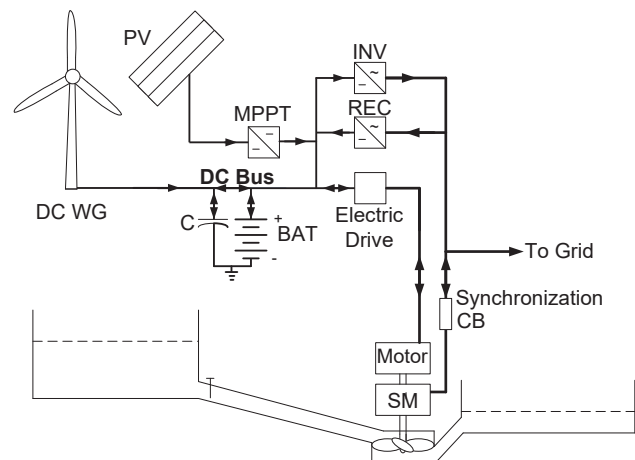


Fig. 3. RHPP configuration with combined use of hydro generator and motor

The same axial shaft that connects the Francis hydro turbine (FT) impellers can be coupled with the electric motor. The resulting mechanical power would then be used to pump water without the need to start SM using grid power (thus eliminating the grid starting currents problem). Such combination would also allow DC to AC conversion through the synchronous generator.

The synchronous generator would provide pure sine wave current with minimum harmonics. Through the DC voltage/current control of its field excitation, SM would offer a wide operating range of power factor along with precise

power factor control. This would serve a desirable positive impact on the utility AC grid, through the possibility of generating additional reactive power, if required by the grid, with magnitudes higher than the inverters can provide. At the same time, the grid would also benefit from the generator rotational inertia, and as can be seen from (1) by increasing the kinetic energy reserve.

By allowing off-grid starting and operating of the PSPP, with isolation from the AC grid, undesirable transient grid loads are eliminated. Moreover, once synchronous speed is attained, proper synchronization to the AC grid can take place, followed by a gradual increase or decrease in AC line loads/currents. This also allowed the pumping load control/sharing between the AC grid and the DC bus.

Of course, at the same time, the possibility of the pumped storage power plant work according to the classical scheme is retained.

This configuration allows different working modes of the motor-generator couple in such RHPP during water pumping.

Pumping mode 1. SM is in the motor mode, draining partially its power from the AC grid as the DC bus powered motor shares the water-pumping load.

$$P_p = P_M^+ + P_{SM}^- \quad (2)$$

where P_p – load power in the motor mode; P_M^+ – DC power, consumed by the motor, $P_M^+ < P_p$; P_{SM}^- – AC power input, consumed by the SM in the motor mode.

Pumping mode 2. SM is in the regenerative mode, delivering its power to the AC grid. The DC bus powered motor provides the sources of power to SM and to the water pumping load, $P_M^+ > P_p$.

$$P_p = P_M^+ - P_{SM}^- \quad (3)$$

Generating mode. Water flowing down the hydro storage is used to rotate FT along with the DC bus powered motor. All of them together drive the rotor of the SM, which is supplying its power to the AC grid.

$$P_{SM}^- = P_M^+ + P_H, \quad (4)$$

where P_{SM}^- – AC power output to the grid, provided by the SM in the generator mode; P_M^+ – DC power, consumed by the motor; P_H – power from FT.

The problem is the choice of the type of motor that provides the optimum performance of the proposed scheme.

4. 4. Selection of DC bus powered motor type

Taking into account the above modes, we can set up selection criteria for the DC bus powered motor, assessing pros and cons of each possible motor type (Table 1).

The DC motor offers the possibility to be directly powered from the DC bus. The DC motor can work as a motor as well as a generator, which allows it to charge the batteries from the hydro mechanical power or even from the AC grid when the PSPP is operated in the pumping mode.

DC motors, however, have a relatively low efficiency up to 90 % at optimum load for medium power machines [15], also necessitates regular maintenance to replace brushes and even commutation. Though this problem can be solved by using brushless type DC motors with special drives, in general, however, relatively high cost, as well as uncommon availability, makes DC motors an unattractive solution for RHPP.

Table 1

Motors comparison for selection

Parameter	DC motor	PM motor	Synchronous motor	Induction motor
Efficiency as motor	Up to 90 %	Up to 95 %	98–99 %	96–97.5 %
Technology	Very mature	Mature	Very mature	Very mature
Availability in high ratings	Limited	Rare	Widely available	Widely available
Relative cost	High	Very high	Low	Low
Maintenance frequency & cost	High	Low	Low	Minimum
Manufacturing future cost reduction	Saturated	Promising	Saturated	Saturated
Operates as generator	Yes	Yes	Yes	Yes
Requires external power drive	Minimum	Yes	Yes	Yes
Power speed curve	Linear	Linear	Complex (when out of synch.)	High steep

Similar to the DC motor above, the brushless permanent magnet motor (PM) also offers the possibility to work as both motor and generator. This allows it to charge the batteries from the hydro mechanical power or even from the grid when the hydro storage power SG operates in the motor mode (powered from the AC grid). PM offers high efficiency [16]; however, its present limited use due to relatively low power ratings and the high cost of its magnets makes it an unattractive present solution.

It also can work as both motor and generator. Its mature technology, availability in high power ratings and relatively competitive prices make it worth being taken into consideration.

The synchronous motor has very high efficiency as a generator and as a motor of around 98–99 % by some reputed manufacturers (such as ABB) [17], and its power factor can be controlled to suite optimum requirements using its DC excitation control. However, it has some drawbacks. The synchronous motor suffers from transient instability (out of synchronism) when transient mechanical torque exceeds the electrical power input, which is compensated by the presence of damper winding inside the rotor. In addition, the synchronous motor will require a DC to AC drive for controlling its speed and its power output. It would provide the best efficiency combination with variable frequency drives (VFD), and can be a promising future solution if deeply researched.

The induction motor (IM) also offers the possibility to work as a generator if it was customized to have its rotor d&q windings fed with externally controlled AC voltage sources, which would offer controlled charging through variable voltage and frequency output independently of the constant rated RPM speed. However, this feature would not be required and can be left as an option. Modern VFD from well-reputed suppliers, such as Siemens, are available on the market, which offer power recovery feature allowing easy recovery of standard IM excessive power back to the DC bus [18].

The standard IM, therefore, offers a simple power supply scheme and has high efficiency of around 96–97.4 % by some

reputed manufacturers (such as Siemens) [19]. In addition, its remarkable slip torque speed curve at rated speed can be exploited to offer certain additional advantages.

The IM cannot be operated directly from the DC bus except through the VFD. However, the VFD systems that have been widely used since the last quarter of the 20th century, offered at a competitive price and high efficiency, gives a great advantage in power and control and counters the balance in favor of standard IM.

The IM has the drawback of low power factor and high currents during start up, these, however, do not offer a challenge. The modern VFD gives soft starting characteristics, also three phase VFD allows the modes of forward phase rotation (needed during pumped storage discharge) and reverse phase rotation (needed during the pumping mode) without the need of changeover phase reversing contactors.

High efficiency, brushless design, proven reliability, mature technologies and wide availability at the most competitive prices for high power ratings make IM at present the best choice for the motor in the proposed RHPP scheme.

5. Analysis of induction motor favorable performance

The IM inherited unique characteristic of the torque slip curve (Fig. 4) [20, 21] offers a major advantage through the significant change in torque for any slight variation in rotational speed. Thus, if well exploited, IM can act in favor of grid frequency regulation when operated at a constant VFD frequency, releasing almost instantly extra power when grid frequency drops, as well as reducing almost instantly the power output when grid frequency rises. IM can improve grid frequency reliability by trying to maintain stability that opposes undesirable fluctuations, acting as dynamic frequency control support.

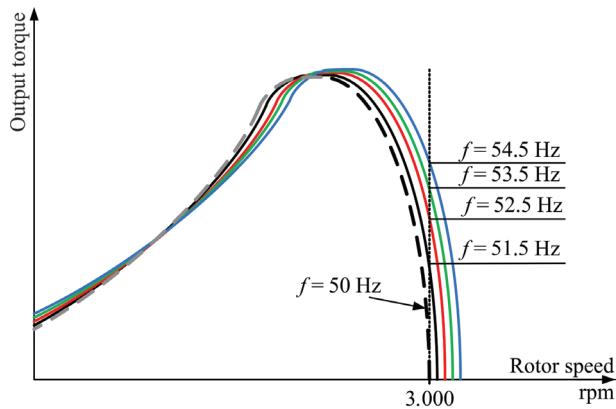


Fig. 4. Torque slip curve of induction motor

Confirmation of the effect of this torque slip on the expected IM dynamic properties is the necessary key to proof of the proposed RHPP scheme. In the work, the well-known mathematical model of 3 phase asynchronous electric machine is used [22].

Stator 3 phase unity input voltages of IM U_a, U_b, U_c :

$$\begin{aligned} U_a &= 1.41 \sin \omega_0 t, \\ U_b &= 1.41 \sin(\omega_0 t - 2\pi/3), \\ U_c &= 1.41 \sin(\omega_0 t + 2\pi/3), \end{aligned} \quad (5)$$

where ω_0 – input voltages angular frequency, $\omega_0 = 2\pi f$; f – power system frequency.

The constant component of the stator windings inductance L_{st} :

$$L_{st} = L_a = L_b = L_c = (L_0 + L_d + L_q)/3, \quad (6)$$

where L_a, L_b, L_c – stator windings inductance in phases; L_0 – zero-sequence inductance; L_d, L_q – stator windings inductance on longitudinal and transverse axes.

Mutual inductance of stator windings M_{st} :

$$M_{st} = m_0 = \frac{1}{3} \left(L_0 - \frac{L_d + L_q}{2} \right), \quad (7)$$

where m_0 – constant component of mutual inductance of stator windings.

Mutual inductance between rotor and stator windings M_1 :

$$\begin{cases} M_{1da} = M_{1dm} \cos \omega_0 t; \\ M_{1db} = M_{1dm} \cos(\omega_0 t - 2\pi/3); \\ M_{1dc} = M_{1dm} \cos(\omega_0 t + 2\pi/3); \\ \\ M_{1qa} = M_{1qm} \sin \omega_0 t; \\ M_{1qb} = M_{1qm} \sin(\omega_0 t - 2\pi/3); \\ M_{1qc} = M_{1qm} \sin(\omega_0 t + 2\pi/3), \end{cases} \quad (8)$$

where M_{1qm}, M_{1dm} – amplitude (maximum) value of mutual rotor windings inductance on longitudinal and transverse axes.

Rotor currents on longitudinal and transverse axes i_1 :

$$\begin{cases} i_{1d} = \int -\omega_0 \frac{R_{1d} i_{1d}}{L_{1d}} dt - \frac{M_{1da} i_a + M_{1db} i_b + M_{1dc} i_c}{L_{1d}}, \\ i_{1q} = \int -\omega_0 \frac{R_{1q} i_{1q}}{L_{1q}} dt - \frac{M_{1qa} i_a + M_{1qb} i_b + M_{1qc} i_c}{L_{1q}}, \end{cases} \quad (9)$$

where R_{1d}, R_{1q} – rotor windings resistance on longitudinal and transverse axes; L_{1d}, L_{1q} – rotor windings inductance on longitudinal and transverse axes.

Stator currents i :

$$\begin{cases} i_a = \int \omega_0 \frac{U_a - R_{st} i_a}{L_{st}} dt - \frac{M_{st} i_b + M_{st} i_c + M_{1d} i_d + M_{1q} i_q}{L_{st}}, \\ i_b = \int \omega_0 \frac{U_b - R_{st} i_b}{L_{st}} dt - \frac{M_{st} i_a + M_{st} i_c + M_{1d} i_d + M_{1q} i_q}{L_{st}}, \\ i_c = \int \omega_0 \frac{U_c - R_{st} i_c}{L_{st}} dt - \frac{M_{st} i_a + M_{st} i_b + M_{1d} i_d + M_{1q} i_q}{L_{st}}, \end{cases} \quad (10)$$

where R_{st} – stator winding resistance (equal for all phases); M_{1q}, M_{1d} – mutual inductance of stator windings on longitudinal and transverse axes.

Rotor angular speed ω_r :

$$\omega_r = \omega_{r0} + \Delta\omega; \quad (11)$$

$$\Delta\omega = \frac{\omega_0}{M_{in}} \int (P - P_{ls} - P_{ld}) dt, \quad (12)$$

where ω_{r0} – synchronous rotor speed; $\Delta\omega$ – rotor speed deviation from synchronous; M_{in} – total moment of inertia of IM; P – instant power of IM; P_{ls}, P_{ld} – static and dynamic load moment.

IM instant power:

$$P = U_a i_a + U_b i_b + U_c i_c. \quad (13)$$

The IM for small scaled RHPP in the model is set by the below parameters: $f=50$ Hz; $\omega_0=314$ (to cover the slip and rotate at 314 rad/s); $L_d=L_q=0.5$; $L_0=0.06$; $M_{1qm}=M_{1dm}=0.3$; $L_{1d}=L_{1q}=0.43$; $R_{st}=0.03$; $R_1=0.03$; $P_b=0.02$; $P_{ld}=0.63$; $M_m=1.1$.

Fig. 5 shows the results of Matlab Simulink simulation of the output mechanical power P^* response (in normalized values) of the SM-coupled IM for a sudden grid frequency f variation. The motor is fed by an independent constant frequency source (representing the DC bus fed VFD output).

An increase of 0.4 % (0.2 Hz) in grid frequency f results in around 13 % drop in IM power P^* , i. e. SM power exported to the grid, until the IM rotational speed and grid frequency return to the nominal steady-state value. A decrease of 0.4 % in rotational speed results in around 13 % increase in motor power, until the rotational speed returns to its normal value. An increase of 0.8 % (0.4 Hz) in f results in around 25 % drop in P^* , a decrease of 0.8 % in f results in around 25 % increase in P^* , until the rotational speed returns to its nominal value. The duration of the transition process is within 0.1 s in both cases.

The simulation results confirm the response expected from understanding the torque slip curve of the IM. Small variations in the grid frequency result in fast significant changes in the IM output power, as a dynamic reaction that opposes variations in the grid frequency. Thus, this supports expectations for the stable frequency regulation offered by the proposed configuration.

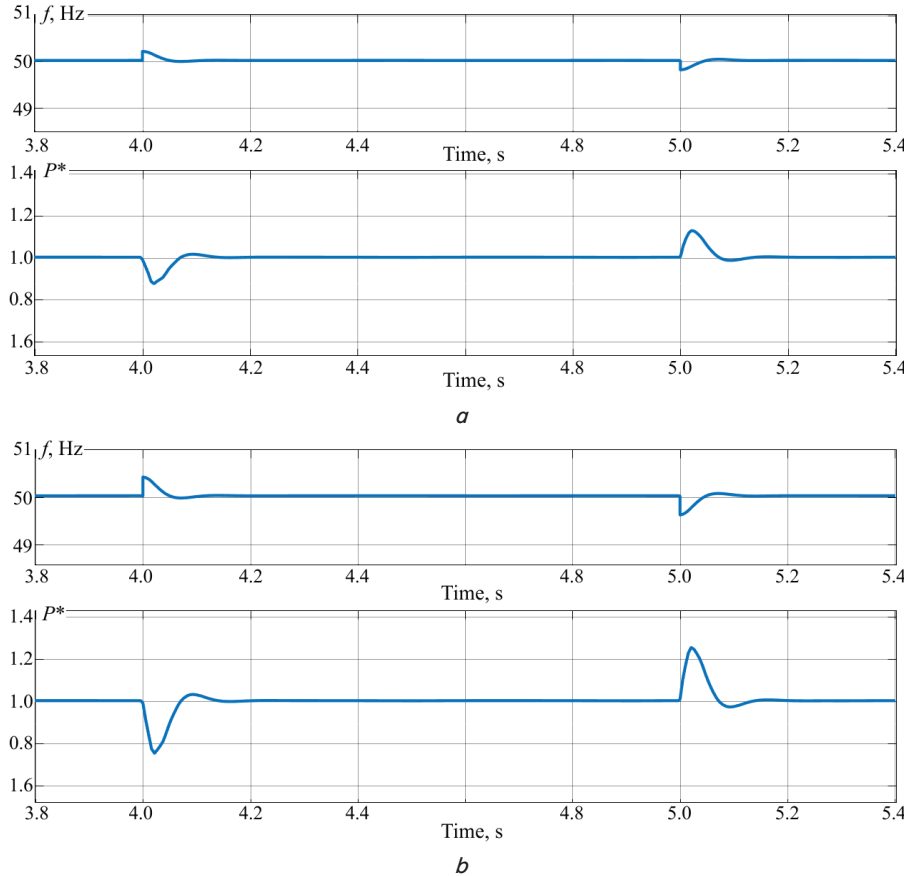


Fig. 5. Transient process for SM-coupled IM response to the grid frequency variation: a – 0.4 % of grid frequency; b – 0.8 % of grid frequency

If, however, higher drops in frequency occur (in unreliable grids), the power of the IM would depend on the maximum torque it can deliver, until VFD protection is activated. Further, the control and monitoring logic used in coordination with the VFD will drop accordingly the supply frequency output to maintain the output power within certain limits without overloading the VFD nor the DC bus.

Similarly, if grid frequency overrun occurs at higher levels, the IM would stop acting as a load, and reverse power will start flowing backwards. IM could be used to act as automatic energy recovery towards the DC bus, unless the same monitoring and control logic coordinates with the VFD to increase its output frequency to prevent reverse power.

In view of the above, the desirable dynamic response is achieved with minimum feedback control due to the inherited features of IM, offering very promising features towards system frequency stability.

6. Assessment of the feasibility of using VFD instead of grid inverter

In the proposed RHPP scheme, the IM with VFD partially replaces the inverter and can even eliminate the need for its use. However, it is known that modern inverters have very high efficiency. To confirm the possibility of obtaining economic benefits from a larger share of RE in the power system with such RHPP, it is necessary to analyze the ratio of the efficiency of systems with VFD and inverter. For this, typical daily generation and load profiles, an example of which is shown in Fig. 6 (based on normalized data for June 2017 from [23, 24]) can be used. Here, for the megawatt-class RHPP under consideration, it is set that the ratio of PV and WG power is 1:3, the power of VFD and IM is equal to the power of the pumped storage unit, which is 90 % of the total power of PV and WG.

The day may be divided into 5 periods based on the location of the graphs intersection points in Fig. 6.

Periods I&V: Low RE output power with higher power demand, requiring PSPP to compensate for generation shortage.

Period II: Short duration of low RE output power with slightly lower demand, which may not necessitate PSPP to operate in the storage mode. Excess power may be stored in the DC storage batteries.

Period III: The RE output power and load demand are almost matching, not necessitating PSPP to deliver nor store power. Small energy fluctuations are compensated by the DC storage batteries.

Period IV: The RE output power significantly exceeds the load and allows PSPP to operate in the storage mode for the full use of RE.

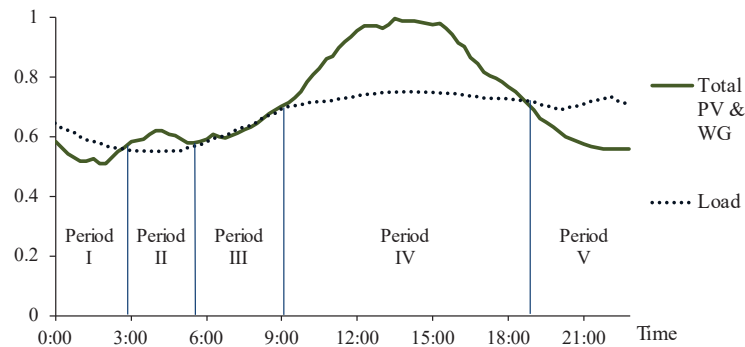


Fig. 6. Example of daily RHPP generation and load profiles in June

Table 2 below shows the values of the RHPP elements efficiency used for calculations. The inverter efficiency is given by [25], and the VFD by [26].

Table 2

Parameters of RHPP elements

Parameter	Inverter	VFD	IM	SM (motor)	SM (generator)
Efficiency, %	98.8	98.5	97.4	98.2–99	99
Hardware cost	More	Less			

Table 3 shows the efficiency of electrical systems used for DC to AC conversion for RE output to the grid and for PSPP water pumping calculated for the traditional (Fig. 1) and proposed (Fig. 3) RHPP schemes. For the traditional RHPP scheme, the efficiency of electrical energy conversion when power is output to the grid is equal to the inverter efficiency: 98.8 %, and the efficiency of the inverter-SM system when pumping water is $98.8 \times 98.2 = 97.02$ %. For the proposed RHPP scheme, the efficiency of the VFD-IM-SM system when power is output to the grid is $98.5 \times 97.4 \times 99 = 94.98$ %, and the efficiency of the VFD-IM system when pumping water is $98.5 \times 97.4 = 95.94$ %.

Table 3

Efficiency of electrical systems in traditional and proposed RHPP scheme

Period	System efficiency, %			
	Inverter-SM system		VFD-IM-SM system	
	To grid	Pumping	To grid	Pumping
I, III & V	98.8	–	94.98	–
IV	98.8	97.02	94.98	95.94
II	98.8	–	94.98	–

As can be seen from Table 3, in all periods the efficiency of the VFD-IM-SM system is 1–4 % lower than that of the inverter-SM system. However, the greatest difference in efficiency falls on periods I–III & V, when the generated RE power does not exceed 70 % of the installed capacity. Thus, in absolute terms, the increase in losses in case of using the VFD-IM-SM system instead of the inverter is no more than 2.7 % of the installed capacity.

At the same time, the proposed RHPP scheme using the VFD-IM-SM system for RE output to the grid and for PSPP water pumping provides a significant advantage in solving problems that limit the allowable share of RE in the power system. The technical solutions and equipment used in it are well known and widely used, have a relatively low cost and are re-

liable in operation. Thus, they are free from the disadvantages of the known solutions that electronically mimic the rotational inertia of conventional generators or use powerful electrochemical batteries. The presence of hydraulic accumulation, as well as significant spinning kinetic inertia and the ability to stabilize the frequency of the IM-SM-FT system allow further increase in the share of RE sources in the power system without threatening its stability. With that, an increase in the share of cheap energy from RE will make it possible to compensate for the lower efficiency of the proposed RHPP scheme.

The equipment of leading manufacturers available on the market allows the implementation of the proposed RHPP scheme with a rated power of tens of megawatts. However, the creation of RHPP based on PV and WG with lower rated power seems to be inexpedient due to the complexity of the construction of the corresponding PSPP. Certainly, the presented calculations were made as a first approximation and are estimated. A more detailed justification of the proposed solution effectiveness requires further comprehensive modeling of possible plant operation modes.

7. Conclusions

1. As a result of comparison of various renewable hybrid power plant schemes comprising PV, WG and PSPP, it was determined that a rational configuration of a RHPP contains an induction motor coupled by the same shaft with a pumped storage unit synchronous generator and turbine. The induction motor is connected through a variable frequency drive to a photovoltaic and wind generators common DC bus. This solution increases the utilization rate of the installed capacity of PSPP equipment and allows obtaining a greater share of energy from renewable energy sources.

2. The results of the simulation of the response of IM connected to the DC buses through the VFD to various changes in the rotational speed showed that in the proposed RHPP scheme a grid frequency dynamic control is achieved in a wide range of disturbances. The considerable rotational inertia of the IM-SM-TF system has a positive effect on power system stability. In addition, the use of the VFD-IM-SM system eliminates the influence of higher harmonics on the power grid by reducing the rated capacity of grid inverters and minimization of their use. Comparison of the inverter efficiency and the efficiency of the DC/AC conversion using the VFD-ID-SM system showed their proximity, but with the inverter advantage. However, the creation of the RHPP of the proposed scheme makes it possible to eliminate the obstacles to a further increase in the share of renewable energy in the overall energy balance.

References

1. Delille G., Francois B., Malarange G. Dynamic Frequency Control Support by Energy Storage to Reduce the Impact of Wind and Solar Generation on Isolated Power System's Inertia // IEEE Transactions on Sustainable Energy. 2012. Vol. 3, Issue 4. P. 931–939. doi: <https://doi.org/10.1109/tste.2012.2205025>
2. Lippert M. Optimizing energy storage systems for large wind and solar plants. Saft document. 2017. No. 21989-1117-2. URL: <http://www.renewableenergyworld.com/white-papers/2018/01/optimizing-energy-storage-systems-for-large-wind-and-solar-plants.html>
3. Dudurych I. M. Statistical analysis of frequency response of island power system under increasing wind penetration // IEEE PES General Meeting. 2010. doi: <https://doi.org/10.1109/pes.2010.5588079>
4. Kundur P. Power System Stability and Control. McGraw-Hill, 1994. 1176 p.
5. Bomer J. All Island TSO Facilitation of Renewables Study – Final Report for Work Package 3 Ecofys // Tech. Rep. 2010.
6. A Wind-Hydro-Pumped Storage Station Leading to High RES Penetration in the Autonomous Island System of Ikaria / Papaefthymiou S. V., Karamanou E. G., Papathanassiou S. A., Papadopoulos M. P. // IEEE Transactions on Sustainable Energy. 2010. Vol. 1, Issue 3. P. 163–172. doi: <https://doi.org/10.1109/tste.2010.2059053>
7. Brown P. D., Peas Lopes J. A., Matos M. A. Optimization of Pumped Storage Capacity in an Isolated Power System With Large Renewable Penetration // IEEE Transactions on Power Systems. 2008. Vol. 23, Issue 2. P. 523–531. doi: <https://doi.org/10.1109/tpwrs.2008.919419>
8. Delille G., Francois B., Malarange G. Dynamic frequency control support: A virtual inertia provided by distributed energy storage to isolated power systems // 2010 IEEE PES Innovative Smart Grid Technologies Conference Europe (ISGT Europe). 2010. doi: <https://doi.org/10.1109/isgteurope.2010.5638887>
9. Kayikci M., Milanovic J. V. Dynamic Contribution of DFIG-Based Wind Plants to System Frequency Disturbances // IEEE Transactions on Power Systems. 2009. Vol. 24, Issue 2. P. 859–867. doi: <https://doi.org/10.1109/tpwrs.2009.2016062>
10. Yingcheng X., Nengling T. Review of contribution to frequency control through variable speed wind turbine // Renewable Energy. 2011. Vol. 36, Issue 6. P. 1671–1677. doi: <https://doi.org/10.1016/j.renene.2010.11.009>
11. Ekanayake J., Jenkins N. Comparison of the Response of Doubly Fed and Fixed-Speed Induction Generator Wind Turbines to Changes in Network Frequency // IEEE Transactions on Energy Conversion. 2004. Vol. 19, Issue 4. P. 800–802. doi: <https://doi.org/10.1109/tec.2004.827712>
12. Miller J. M. Electrical and Thermal Performance of the Carbon-carbon Ultracapacitor Under Constant Power Conditions // 2007 IEEE Vehicle Power and Propulsion Conference. 2007. doi: <https://doi.org/10.1109/vppc.2007.4544186>
13. Atcitty S. Electrochemical Capacitor Characterization for Electric Utility Applications. Blacksburg, 2006.
14. Stahlkopf K. Taking wind mainstream // IEEE Spectrum. 2006. URL: <https://spectrum.ieee.org/energy/renewables/taking-wind-mainstream>
15. Issa H. Separately Excited DC Motor Optimal Efficiency Controller // International Journal of Engineering and Innovative Technology (IJEIT). 2013. Vol. 3, Issue 1. P. 533–539.
16. Chau K. T., Chan C. C., Liu C. Overview of Permanent-Magnet Brushless Drives for Electric and Hybrid Electric Vehicles // IEEE Transactions on Industrial Electronics. 2008. Vol. 55, Issue 6. P. 2246–2257. doi: <https://doi.org/10.1109/tie.2008.918403>
17. Rosberg J. ABB reaches 99.05% efficiency, the highest ever recorded for a synchronous motor // ABB Conversations. 2017. URL: <https://www.abb-conversations.com/2017/07/abb-motor-sets-world-record-in-energy-efficiency>
18. Prachyl S. Variable Frequency drives and Energy Savings. It's more than just fan and pump applications // Siemens. 2010. URL: https://www.appliedc.com/wp-content/uploads/2017/05/VariableFrequencyDrives_WhitePaper.pdf
19. LOHER VARIO High Voltage Motors // Siemens. 2015. URL: <https://w3app.siemens.com/mcms/infocenter/dokumentencenter/ld/InfocenterLanguagePacks/catalog-d83-2/loher-vario-high-voltage-motors-catalog-d83-2-2015-en.pdf>
20. Caprio M. T., Buckner G. D., Weldon W. F. Controlling the torque-speed characteristics of a polyphase induction motor using a switched rotor ballast network // Proceedings of the 2001 American Control Conference. (Cat. No. 01CH37148). 2001. doi: <https://doi.org/10.1109/acc.2001.945529>
21. New Relation to Improve the Speed and Torque Characteristics of Induction Motors / Mier-Quiroga L. A., Benítez-Read J. S., López-Callejas R., Segovia-de-los-Ríos J. A. // Rev. fac. ing. univ. Antioquia. 2015. Issue 74. P. 37–49. URL: <http://www.scielo.org.co/pdf/rfiua/n74/n74a04.pdf>
22. Mohan N. Advanced Electric Drives: Analysis, Control and Modeling Using Simulink. Minneapolis, 2001.
23. Solarenergie Hochrechnung. URL: <https://www.netztransparenz.de/Weitere-Veroeffentlichungen/Solarenergie-Hochrechnung>
24. NEK Ukrenego Ukraine electricity consumption curved on June 23, 2017. URL: <https://ua.energy/activity/dispatch-information/daily-electricity-production-consumption-schedule>
25. ABB ABB central inverters PVS800 – 500 to 1000 kW. URL: https://library.e.abb.com/public/4736ece73ecf4e3aa2bb7a6e-c7f0ee6d/PVS800_central_inverters_flyer_3AUA0000057380_RevN_EN_lowres.pdf
26. Sinamics Perfect Harmony GH180 // Siemens. 2016. URL: <https://www.industry.siemens.com/drives/global/en/converter/mv-drives/Documents/technical-data-sheets/sinamics-perfect-harmony-gh180-technical-data-en.pdf>